Journal of Energetic Materials
Publication details, including instructions for authors and subscription information:
http://www.informaworld.com/smpp/title~content=t713770432

Binary Phase Diagram Series: HMX/RDX

Robert L. Mckenney; Thomas R. Krawietz

To cite this Article Mckenney, Robert L. and Krawietz, Thomas R.(2003) 'Binary Phase Diagram Series: HMX/RDX', Journal of Energetic Materials, 21: 3, 141 — 166
To link to this Article: DOI: 10.1080/716100385
URL: http://dx.doi.org/10.1080/716100385

Energetic Materials, 21: 141–166, 2003

ISSN: 0737-0652 print
DOI: 10.1080/07370650390256656

Taylor & Francis
Taylor & Francis Group

Binary Phase Diagram Series: HMX/RDX

ROBERT L. McKENNEY, Jr.

THOMAS R. KRAWIETZ

Air Force Research Laboratory
Munitions Directorate, Energetic Materials Branch
Eglin AFB, FL, USA

Two binary phase diagrams for the hexahydro-1,3,5-trinitro-1,3,5-triazine (RDX)/octahydro-1,3,5,7-tetranitro-1,3,5,7-tetrazocine (HMX) system have been determined experimentally. Liquidus curves have been predicted computationally for RDX and δ-HMX. Mixtures exhibit the thermal characteristics associated with simple binary eutectic systems affected by observable HMX polymorphism. The presence of both the β- and δ-polymorphs of HMX were confirmed by X-ray diffraction analysis. The RDX melting temperatures are consistent with calculated liquidus temperatures. Other experimental endothermic processes observed during this investigation are believed to be associated with the melting of binary eutectic compositions involving the β-HMX (188.5 ± 0.3° C/74.9–75.5 mol% RDX) and δ-HMX (191.4 ± 0.4° C/79.0–79.3 mol% RDX) polymorphs and the solid-state transition from the β- to the δ-HMX polymorph.

Keywords: RDX, HMX, phase diagram, eutectics, polymorphs

Introduction

Both RDX (hexahydro-1,3,5-trinitro-1,3,5-triazine) and HMX (octahydro-1,3,5,7-tetranitro-1,3,5,7-tetrazocine) are important energetic materials commonly used in a variety of military explosive compositions. The RDX produced in the United States at the Holston Army Ammunition Plant (HSAAP) by the Bachmann process, hereinafter

Address correspondence to R. L. McKenney Jr., Air Force Research Laboratory, Munitions Directorate, Energetic Materials Branch, Eglin AFB, FL 32542. E-mail: robert.mckenney@eglin.af.mil

designated HRDX, generally contains from 4% to 17% by weight of HMX as an impurity. The RDX used in this investigation, hereinafter designated S-RDX, was produced in France by the Societe Nationale des Poudres et Explosifs (SNPE) by using the Woolwich process, which yields an essentially HMX-free product. HMX, also produced at HSAAP, exists in four solid-state polymorphs that are designated α-, β-, γ-, and δ-HMX. Over the years these polymorphs have been extensively studied [1–4] with respect to crystal properties, solid phase transitions, and sensitivities to external stimuli. The β-polymorph is of primary interest to the military because it has the highest crystal density of the four polymorphs and is the form provided by both HSAAP and SNPE. This investigation was prompted by another study undertaken at this facility to characterize the thermal properties of both HRDX and S-RDX and their mixtures with 2,4,6-trinitrotoluene (TNT) [5]. Besides the dramatic differences in the behavior of the two types of RDX in the One-Liter Test [5,6], it was also observed that their standard DSC thermograms were noticeably different. The S-RDX thermogram exhibits a sharp endothermic event attributed to the RDX melting process at 205.3°C, which is immediately followed by thermal decomposition. The HRDX, on the other hand, exhibits a broad, generally twin-peaked endothermic event that occurs over the temperature range 188–205°C, which is followed by thermal decomposition. An earlier study [7] of the thermal behavior of mixtures of RDX and HMX at high concentrations (70–100% by weight) of the latter found two endothermic events associated with the mixtures. One was observed at a consistent temperature of 187–188°C and the other over the temperature range 199–205°C with the temperature increasing as the RDX concentration was increased to a maximum of 30% by weight. The former event was attributed to RDX melting and the latter to a polymorph transition. The objective of this investigation is to generate the complete temperature/composition diagram and identify the process associated with each endothermic event. Emphasis is placed on the higher concentrations of RDX.

Experimental

Component Liquidus Curve Calculations

Component liquidus temperatures are computationally derived by solving

$$R \ln X = \Delta H_{\text{fus}} \left(-\frac{1}{T} + \frac{1}{T_o} \right), \tag{1}$$

where T is the melting point (K) of a specic composition, T_o, ΔH_{fus} and x are the melting point (K), heat of fusion (cal mol^{-1}), and mol fraction of component A or B, respectively, and R is the gas constant ($1.987\,\text{cal K}^{-1}\,\text{mol}^{-1}$). Experimental melting points associated with the S-RDX component, determined by DSC heating operations on mixtures of the stable polymorphs of both components, were used for comparison with corresponding calculated liquidus values. Such comparison was not possible for the δ-HMX component because of the onset of thermal decomposition immediately after the transition from β-HMX in the presence of RDX.

Differential Scanning Calorimetry. S-RDX, β-HMX, and mixtures thereof were thermally characterized by using a TA Instruments Dual Differential Scanning Calorimeter, Model 912, equipped with a 2100 Thermal Analyzer Data System. Standard aluminum sample pans and lids, TA Instruments part nos. 072492 and 073191, respectively, were used for all melting operations carried out by using the standard Dual Sample DSC cell. Upper temperature limits were applied as required to this binary system to avoid the initiation of thermal decomposition, a process that commences immediately after melting of either of the components and their mixtures. Sample weights were unlimited if only endothermic processes were to be studied and were limited to 0.2 mg for those to be taken to exothermic decomposition. All heating operations were started at 30°C and carried out at a heating rate of 5°C/min with the exception of one operation carried out at 1°C/min. The former heating rate was used in this study in the interest of time.

Multiple heating operations, usually two to four, were carried out on six of the mixtures. Peak temperatures are reported for all endothermic processes unless otherwise specified. Temperatures reported for exothermic processes are the point of deviation from the baseline and are approximate. Mixtures were prepared by grinding weighed portions of dry energetic materials in an agate mortar with a glass pestle to ensure homogeneity. The DSC was calibrated by using indium metal as a temperature and calorimetric standard.

Hot Stage Microscopy. HSM experiments were carried out by using a Mettler Hot Stage, Model FP 82, equipped with an FP 80 central

processor. All observations were made with a Leitz Orthoplan Universal Largefield microscope equipped with a polarizing condenser and high-resolution video system, Javelin Smart Camera, Model JE3762DSP, which was operated at shutter speeds of 1/250 or 1/500 s. All photomicrographs were obtained through a Leitz NPL 10X 0.20P lens (150 ×). The heating rate was 1°C/min, and the cooling rate was uncontrolled. Temperatures are reported as ranges, temperature at which melting is first observed and at which the last crystal melts.

X-ray Diffraction Analysis. X-ray diffraction was performed by using a Philips X'Pert Plus Diffractometer and Cu K_α radiation. A powder sample consisting of approximately 200 µg was sprinkled onto a glass microscope slide that had been covered with double-sided sticky tape. A $\Theta/2\Theta$ scan was performed by using 0.010° fixed divergent and antiscatter slits, and a 0.20° receiving slit.

Results

Thermal Properties of S-RDX and HMX. The S-RDX (lot no. 065S00) used during this investigation prior to any grinding operation was designated Class 5 with a nominal particle size of less than 44 µm. Analysis by high-performance liquid chromatography (HPLC) revealed only a trace of HMX present in the sample. The HMX, National Stock no. 1376-00-865-3964 (lot no. HOL77G240-002), was produced at HSAAP and was designated Class 2 with a nominal particle size of 6–12 µm prior to any grinding operation. No HPLC analysis was carried out with the HMX prior to use. Neither material was subjected to any purification operations, and both are considered to be military grade.

The S-RDX melting point and heat of fusion, 205.3°C and 7356 ± 642 cal/mol, respectively (Lit. 204.1°C and 7886 cal/mol [8]), were obtained by DSC heating operations at 5°C/min. The DSC endothermic event associated with S-RDX melting is a single, relatively symmetric peak that is followed immediately by an exothermic decomposition process. This is in sharp contrast to the endothermic event immediately preceding the exothermic decomposition process associated with HRDX, which in most cases consists of two broad endotherms with peak temperatures in the ranges 188–192 and

203–205°C. The endothermic process associated with S-RDX and the complete thermogram showing exothermic decomposition are presented in Figures 1 and 2, respectively. The complete DSC thermogram associated with the HRDX is shown in Figure 3.

The δ-HMX melting temperature (Lit. 262 and 279°C [1], 278–280°C [9–11], and 280–281°C [8] was not observed under the experimental conditions used during this investigation. A reported heat of fusion is 16,700 cal/mol [12]. An endothermic event was observed, however, in the 195–199°C temperature range that is believed to be associated with the β to δ solid-state phase transition. The peak temperature associated with this endothermic event showed some variation at the 5°C/min heating rate and, as a result, is shown versus sample weight in Table 1 along with scans at 1°C/min. Literature temperatures for this β to δ solid-state transition are 167–183 [13], 183.8 and 168.8 [14], 149–151 [4], and 186.8 [12] °C, and the literature heat of transition is 2350 cal/mol [12]. The transition temperatures from [14] were acquired by DSC experiments at heating rates of 5 and 1°C/min, respectively. The average heat of transition from the DSC experiments carried out during this investigation at a heating rate of 1°C (2190 cal/mol), believed to be the most accurate value, is consistent (6.4% lower) with the literature value. The δ-polymorph, used for a single special experiment during this investigation, was obtained by heating 7.5 and 9.3 mg samples of β-HMX in two separate DSC pans at 5°C/min to 210°C, then allowing the samples to cool to 30°C. Upon reheating a small portion of each sample to 210°C, the DSC thermograms showed no endothermic events. These two samples of δ-HMX were mixed and then subjected to X-ray powder diffraction analysis. The X-ray diffraction patterns of the HMX before and after the polymorph transition are shown in Tables 2 and 3, respectively, and are consistent with literature [15] X-ray diffraction patterns associated with β- and δ-HMX.

DSC Characterization of S-RDX/β-HMX Mixtures. Initial melting operations carried out at a heating rate of 5°C/min with 19 freshly ground mixtures of S-RDX and β-HMX yielded a consistent, endothermic event at an average temperature of 188.5 ± 0.3°C that is believed to be caused by eutectic melting involving β-HMX and S-RDX. The endothermic peak temperatures attributed to S-RDX melting occurred close to its calculated liquidus curve and were immediately followed by exothermic decomposition. In addition to the peaks associated with eutectic melting on the HMX-rich side of the

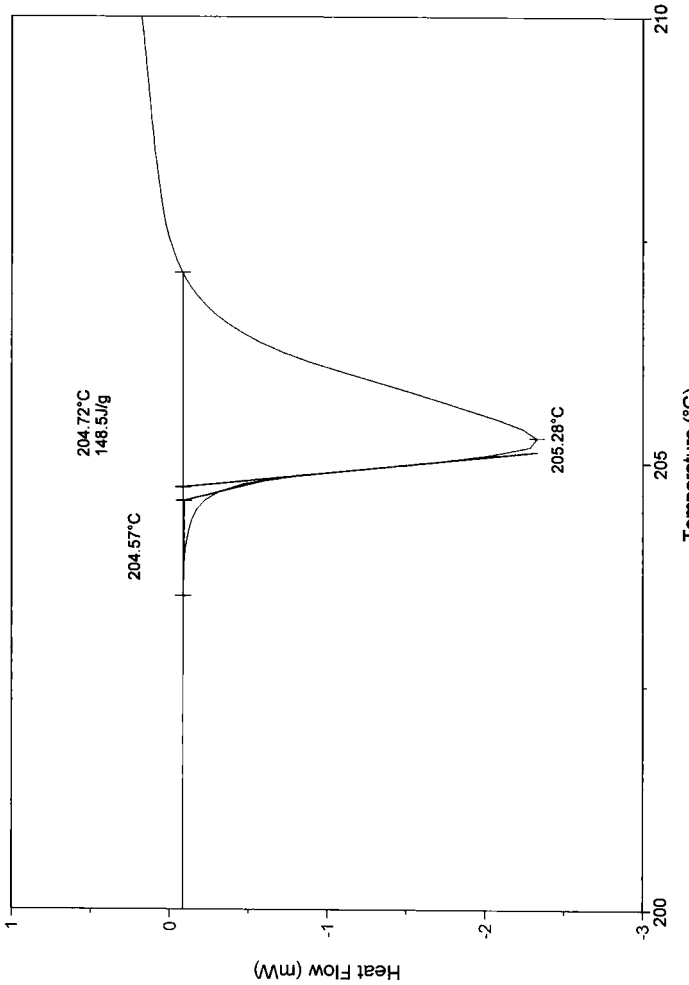

Figure 1. DSC melting endotherm associated with S-RDX.

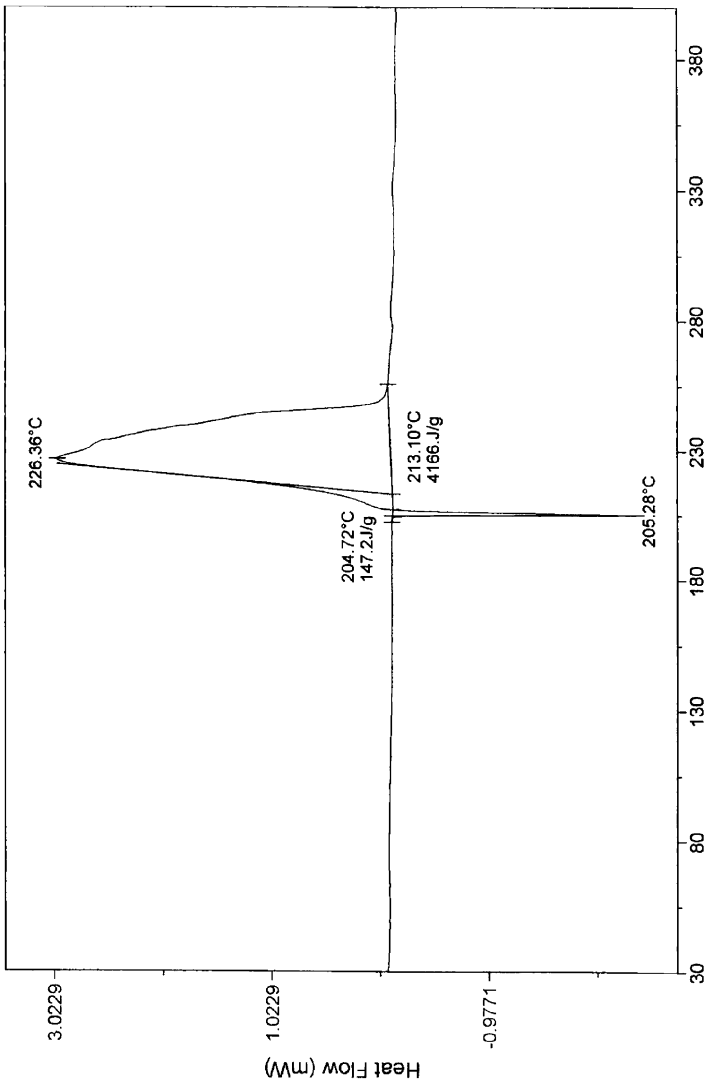

Figure 2. DSC thermogram associated with S-RDX.

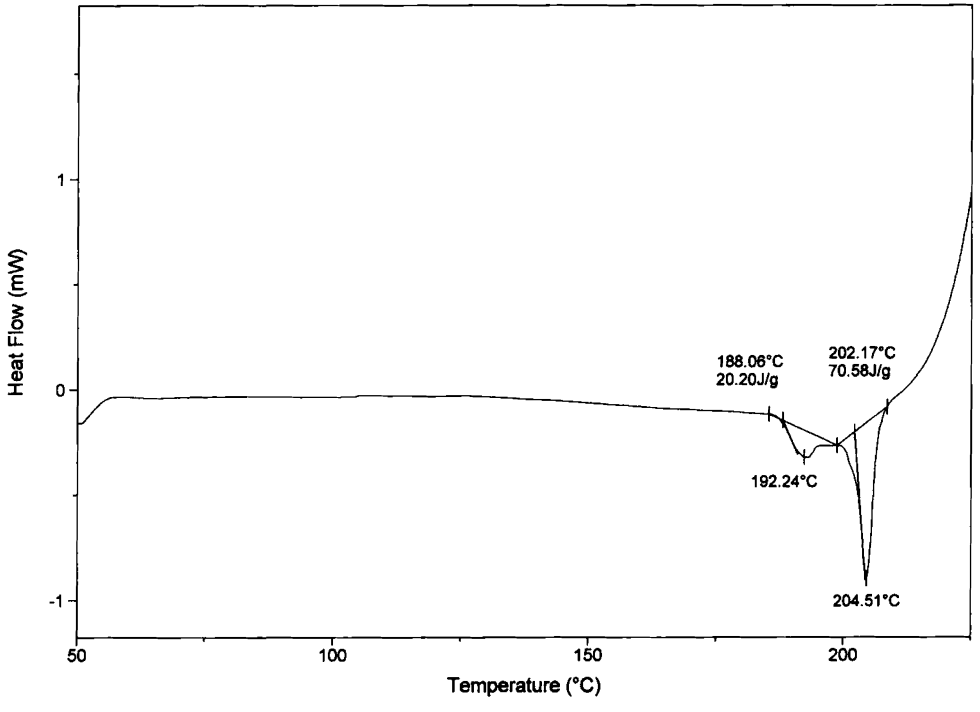

Figure 3. DSC melting endotherms associated with HRDX.

eutectic composition, endothermic peaks were also observed in the temperature range 201.5–203.2°C that are believed to be associated with the β- to δ-HMX solid-state transition. The abrupt increase in this transition temperature in the presence of S-RDX from the 195–199°C temperature range observed with neat HMX is consistent with earlier findings [7] and is believed to result from solid solubility of RDX in β-HMX. This transition process is immediately followed by exothermic decomposition. The data from all (19 compositions) initial melting operations that were taken to thermal decomposition are compiled in Table 4 and shown graphically in Figure 4.

Remelting operations, carried out with mixtures containing 96.8, 92.3, 74.9, 57.1, 36.5, and 12.9 mol% S-RDX, produced a gradual shift of the endothermic event attributed to eutectic melting from an average temperature of 188.5°C to an average temperature of 191.4 ± 0.4°C. This endothermic process is also believed to result from eutectic melting, in this case involving δ-HMX and S-RDX. The data from all (six compositions) remelting operations are compiled in Table 5 and shown graphically in Figures 5 and 6. Included in Figures 4–6 are the approximate temperatures associated with the

Table 1
Endothermic processes associated with the HMX β to δ phase transition

Heating rate (°C/min)	Sample weight (mg)	Enodothermic event		Heat of transition (Kcal/mol)
		Shoulder (°C)	Main peak (°C)	
5	0.2060	–	198.4	2.03
5	0.2080	–	198.8	2.31
5	0.9250	187.5	195.2	1.99
5	0.9270	187.3	195.1	1.99
5	1.5690	–	195.7	2.02
5	1.5730	–	195.6	2.01
5	7.5000	–	198.4	2.05
5	9.3000	–	198.0	1.89
1	3.9640	–	189.6	2.20
1	3.9900	–	188.9	2.18

initiation of thermal decomposition, a process that greatly influences the overall shape of these temperature/composition diagrams.

Calculated Phase Diagram. The liquidus curve for S-RDX was calculated by inserting the measured melting temperature (205.3 ± 0.3 °C) and the experimental heat of fusion (7356 cal/mol) into equation (1). The δ-HMX liquidus curve, calculated by inserting into equation (1)

Table 2
Peak location and relative intensity values for β-HMX

45–1539 β-HMX		Measured	
d-spacing (Å)	Relative intensity(%)	d-spacing (Å)	Relative Intensity(%)
6.0248	39	5.9936	38.6
5.525	41	5.5034	33.4
5.4026	2	5.3702	1.4
4.8536	11	4.8298	9.2
4.3174	100	4.3063	88.4
4.0214	8	4.0143	7.6
3.8627	53	3.8458	51.4
3.4173	23	3.3929	28.7
3.3179	9	3.3058	5.8
3.2779	26	3.2643	25.9
3.1894	11	3.1777	6.9
		3.1114	7.6
3.0637	12	3.0567	13.9
3.0433	6		
3.0124	32	3.004	40.5
2.9436	4	2.9339	1.9
2.8021	71	2.7974	100.0
2.7625	7	2.7519	6.1
2.7013	3	2.691	2.4
2.5467	3	2.5272	2.4
2.4596	2	2.4543	0.6
2.4271	6	2.4187	6.3
2.4108	7	2.4057	4.4
2.2638	2		

Table 3
Peak location and relative intensity values for δ-HMX

44–1622 δ-HMX		Measured	
d-spacing (Å)	Relative intensity(%)	d-spacing (Å)	Relative intensity(%)
6.6779	85	6.6384	83.7
6.5417	32	6.5097	24.4
6.1782	9	6.1415	14.1
5.6872	61	5.6562	65.6
5.4255	69	5.3899	94.7
5.1624	74	5.1346	92.0
4.6617	8	4.6420	30.9
4.2109	38	4.1901	44.6
3.8555	10	3.8403	30.8
3.8287	47	3.8165	46.5
3.8162	47	3.8049	46.1
3.7517	24	3.7410	32.6
3.6330	100	3.6217	100.0
3.4843	66		
3.4748	66	3.4629	56.8
3.3390	8		
3.3215	14		
3.3174	14	3.3093	19.9
3.2708	12	3.2618	15.8
3.1913	66	3.1827	40.0
3.1804	66	3.1662	35.8
3.1428	56	3.1335	47.8
3.0891	5		
2.9710	7		
2.9681	7	2.9614	9.8
2.9261	10	2.9152	12.5
2.8436	4	2.8337	6.4
2.7987	7	2.7904	8.5
2.7128	39		
2.7056	39	2.6968	22.6
2.6379	15	2.6299	9.5
2.5165	23		

(*continued*)

Table 3
Continued

44–1622 δ-HMX		Measured	
d-spacing (Å)	Relative intensity(%)	d-spacing (Å)	Relative intensity(%)
2.5133	23	2.5111	11.7
2.4942	5		
2.4873	5		
2.4584	8	2.4499	4.5
2.4107	5	2.4051	3.0
2.3534	16	2.3488	8.9
2.3475	14		
2.3447	14		
2.2885	6	2.2828	3.0

the literature values for the melting temperature (281.5°C) and heat of fusion (16,700 cal/mol), yielded a curve that intersected the S-RDX liquidus curve at 92.33 mol% S-RDX and 200.4°C. This intersection is consistent with experimental data in that β-HMX does not transition to δ-HMX until the 195–199°C temperature range, and therefore δ-HMX should not exist during initial heating operations until temperatures exceed that range. This calculated intersection was not consistent, however, with the intersection of the calculated S-RDX liquidus curve and the average experimental eutectic melting temperature (79.3 mol% S-RDX/191.4°C) observed during remelting operations. It was assumed and later shown that this higher temperature eutectic does involve δ-HMX and S-RDX. Based on this finding, a notional heat of fusion (9036 cal/mol) was then calculated for δ-HMX by inserting the literature melting temperature (280.5°C) for the neat material, the average measured eutectic melting temperature (191.4°C), the eutectic composition acquired from the intersection of the S-RDX liquidus curve and the average eutectic melting temperature (79.3 mol% S-RDX) into equation (1) and solving for the heat of fusion. This allowed the calculation of the notional δ-HMX liquidus curve that is shown in Figures 5 and 6. To check the validity of this type of heat of fusion calculation, a notional heat of fusion was calculated for S-RDX by using this same technique,

Table 4
Compilation of temperature/composition data associated with initial melting operations (5°C/min) taken to thermal decomposition

	Temperature (°C)			
Mol% S-RDX	β-HMX:S-RDX eutectic	S-RDX melting	HMX ($\beta \rightarrow \delta$)	Exotherm initiation
100	–	205.3	–	207
98.9	188.3	204.4	–	206
97.7	188.2	203.6	–	205
96.8	188.1	202.9	–	204
96.2	188.7	202.2	–	204
92.3	188.7	199.5	–	201
88.4	189.0	196.4	–	199
84.3	188.8	195.6	–	198
80.1	188.7	ND[(1)]	–	195
74.9	189.2/188.6		–	195/195
71.3	188.8		ND[(1)]	200
66.8	188.6		198.5	202
57.1	188.6		200.2	202
52.3	188.4		201.3	204
47.2	188.4		202.3	205
36.5	188.4		202.1	205
30.8	188.3		203.2	205
12.9	188.0		202.8	205
6.56	188.0		201.8	204
2.66	187.7		201.5	206
0	–		198.6	251

[(1)]Not detected.

namely, the measured melting temperatures associated with neat S-RDX (205.3°C) and with the lower temperature eutectic (188.5°C) and a eutectic compositional range (74.9–75.5 mol%) extracted from DSC data. It yielded a value range (7344–7553 cal/mol) that was within 3% of the measured heat of fusion (7356 cal/mol). The S-RDX and δ-HMX liquidus temperature/composition data are shown in Table 6.

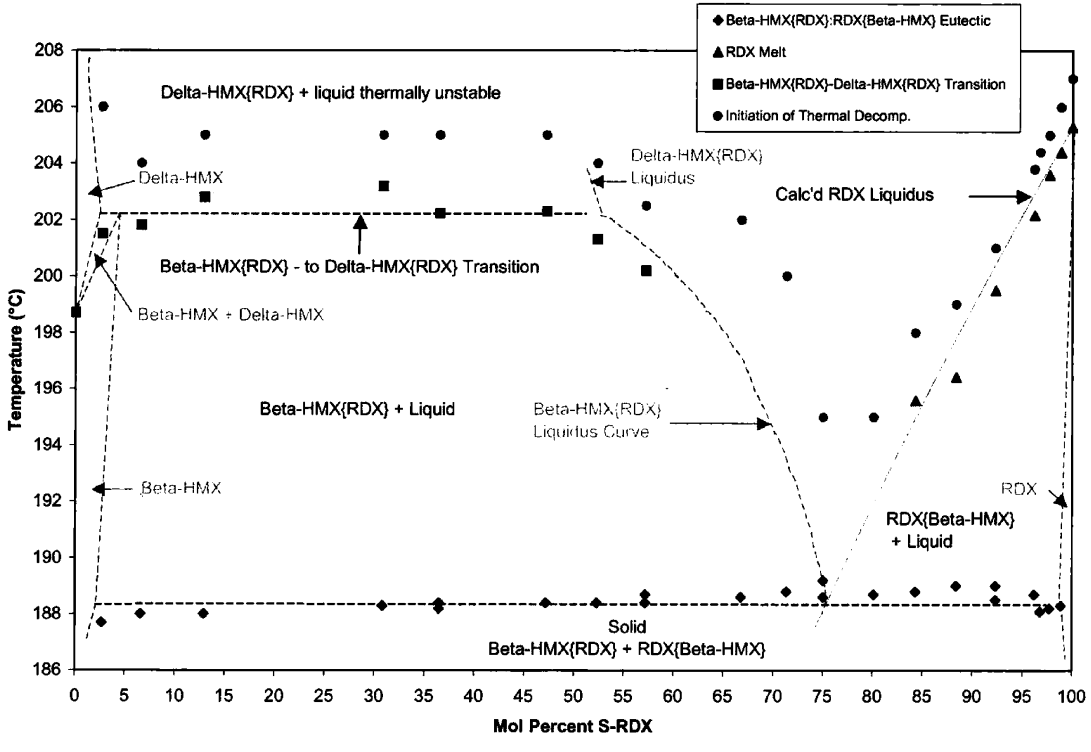

Figure 4. HMX/RDX temperature/composition diagram from initial melting operations.

Table 5
Tabulation of DSC remelting operations

	DSC remelting operations(°C)							
	Initial melting operation		1st		2nd	3rd		
Mol% S-RDX	β-HMX: S-RDX eutectic	HMX $\beta \rightarrow \delta$	β-HMX: S-RDX eutectic	δ-HMX: S-RDX eutectic	δ-HMX: S-RDX eutectic	δ-HMX: S-RDX eutectic	S-RDX melting	Exotherm initiation
96.8	188.1[(1)]	–	ND[(1,2)]	[(3)]	191.1[(4)]	191.1[(5)]	202.9	204
92.3	188.5[(6)]	–	187.8	191.6[(6)]	191.6[(6)]	191.7[(7)]	199.2	200
74.9[(8)]	188.6[(1)]	–		191.8[(4)]	192.2[(6)]	192.0[(9)]	–	197
57.1	188.7[(6)]		188.6	191.1[(6)]	191.7[(6)]	191.6[(7)]	–	194
36.5	188.6[(5)]	201.9	–	190.1[(5)]	–	–	–	–
	188.3[(6,10)]	–	–	–	–	–	–	–
	188.2[(6)]	–	188.1	190.7sh[(6)]	190.9[(6)]	191.2[(9)]	–	196
	188.3[(6)]	–	188.2	190.8sh[(9,11)]	–	–	–	–
12.9	187.9[(6)]	–	188.0[(6)]	–	190.5[(6)]	191.1[(9)]	–	196

[(1)]Heated to 190.5°C then cooled to 30°C.
[(2)]None detected.
[(3)]Heated to 190.5°C, onset temperature for the δ-HMX:S-RDX eutectic was 189.5°C.
[(4)]Heated to 192.5°C then cooled to 30°C.
[(5)]Heated to 210°C.
[(6)]Heated to 194.5°C then cooled to 30°C.
[(7)]Heated to 203°C.
[(8)]At or near β-HMX:S-RDX eutectic composition.
[(9)]Heated to thermal decomposition.
[(10)] Sample removed to check for melting (melting confirmed).
[(11)] Decomposition initiated at 196°C.

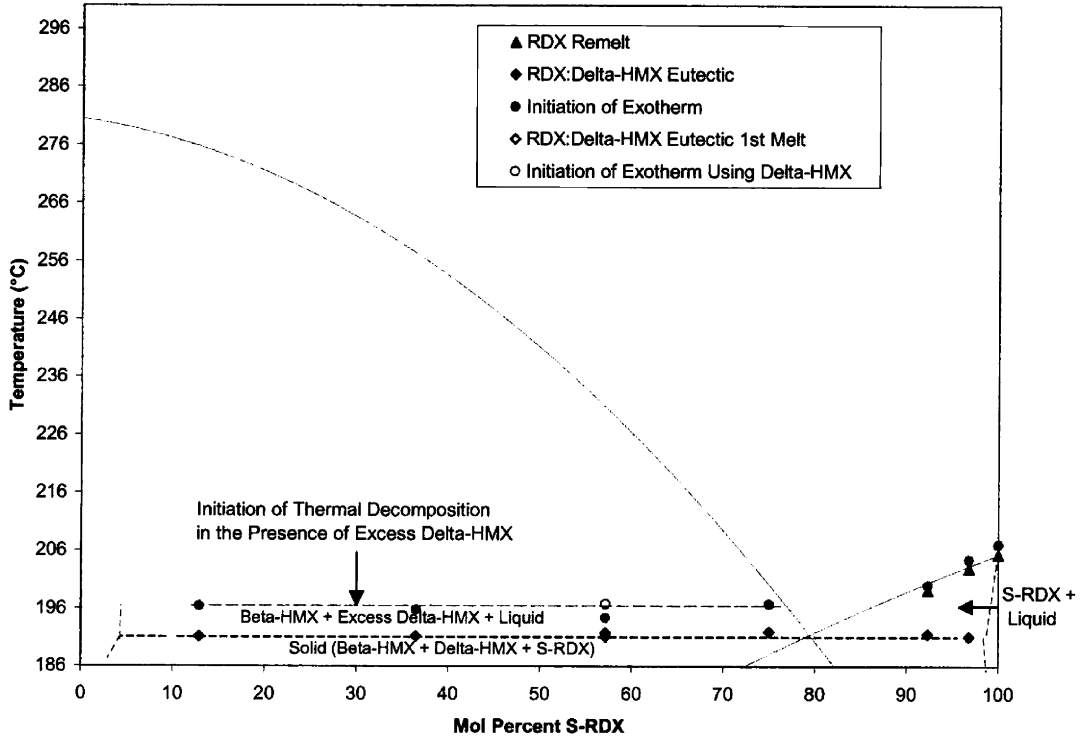

Figure 5. HMX/RDX proposed temperature/composition diagram from remelting operations.

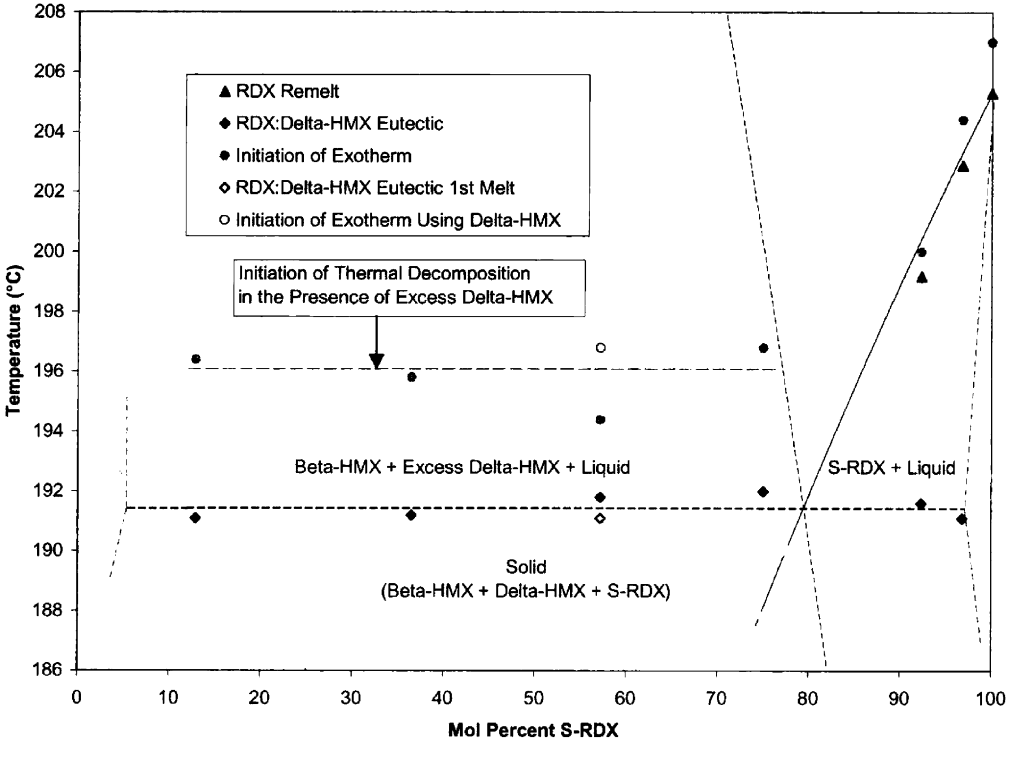

Figure 6. HMX/S-RDX temperature/composition diagram from remelting operations (186–208°C only).

Table 6
Mol%/calculated temperatures used to construct the S-RDX and δ-HMX liquidus curves

	Temperature (°C)		
Mol% S-RDX	S-RDX	δ-HMX[1]	δ-HMX[2]
100.0	205.3	–	–
95.0	202.2	–	189.2
92.4	200.4	–	200.1
92.33[3]	200.4	–	200.4
92.3	200.4	–	200.5
90.0	198.9	–	207.6
85.0	195.5	–	–
80.1	191.9	–	–
80.0	191.9	189.8	227.4
79.9	191.8	190.0	–
79.8	191.7	190.2	–
79.7	191.7	190.5	–
79.5	191.5	190.9	–
79.3[4]	191.4	191.4	–
79.2	191.3	191.6	–
79.1	191.3	191.9	–
79.05	191.2	192.0	–
79.0	191.2	192.1	–
78.8	191.0	192.5	–
78.0	190.4	194.3	–
77.0	189.7	196.5	–
76.0	188.9	198.5	–
75.8	188.8	–	–
75.5[5]	188.5	199.5	–
75.1	188.2	–	–
75.0	188.1	200.5	234.2
73.0	–	204.4	–
70.0	–	209.7	–
65.0	–	217.8	244.7

[1]δ-HMX liquidus temperatures calculated by using 280.5°C melting temperature and 9036 cal/mol heat of fusion.

[2]δ-HMX liquidus temperatures calculated by using 280.5°C melting temperature and 16700 cal/mol heat of fusion.

[3]The calculated eutectic composition and melting temperature using 16,700 cal/mol heat of fusion for δ-HMX.

[4]The calculated eutectic composition and melting temperature using 9036 cal/mol heat of fusion for δ-HMX.

[5]The calculated eutectic composition (intersection of the calculated S-RDX liquidus curve and the average eutectic temperature from initial melting operations).

DSC Characterization of an δ-HMX/S-RDX Mixture (57.1 Mol% S-RDX). A melting operation was carried out in duplicate at a heating rate of 5°C/min with a freshly ground mixture of S-RDX and freshly prepared δ-HMX (57.1 mol% S-RDX) that yielded an endothermic event with an average peak temperature of 191.1°C. This event was followed closely (196.4°C) by exothermic decomposition. This endothermic temperature is consistent with the data (third remelting operation) in Table 5 for the composition with 57.1 mol% S-RDX and suggests this event is correctly identified as a eutectic melting process involving δ-HMX and S-RDX. The DSC thermogram for this operation is shown in Figure 7.

HSM Characterization of an β-HMX/S-RDX Mixture (74.9 Mol% S-RDX). The objective of HSM heating operations, carried out at a heating rate of 1°C/min on a single binary mixture that is believed to be at or near the eutectic composition involving β-HMX and S-RDX, was to verify that the DSC endothermic processes occurring at 188 and 191°C were actually solid-to-liquid transitions. The initial heating operation was characterized by a single melting process that began at approximately 188°C and was complete by 190°C. The heating process was stopped at 190°C and allowed to cool to ambient temperature in order to minimize thermal decomposition. The melted sample contained excessive gas bubbles that may have resulted from either trapped air or from minimal thermal decomposition. The temperature range associated with this initial melting process was consistent with the temperature range obtained from a single DSC operation at 1°C/minute on a mixture containing 57.2 mol% S-RDX (187.8–190°C (189.4°C peak). The second remelting operation on this same sample was initiated by ramping the sample to 180°C and then proceeding at a heating rate of 1°C/minute. The sample darkened during the heating process, but prior to remelting, indicating further recrystallization of the mixture. The remelting process was first observed at 190°C and was not quite complete at 192°C, the temperature at which the heating process was stopped because of the obvious initiation of thermal decomposition. Even though external heating was terminated, the sample continued to decompose thermally until the entire sample was consumed. The higher temperature range associated with this remelting process is consistent with that found during DSC remelting operations where the lower temperature eutectic melting event shifted to a higher temperature

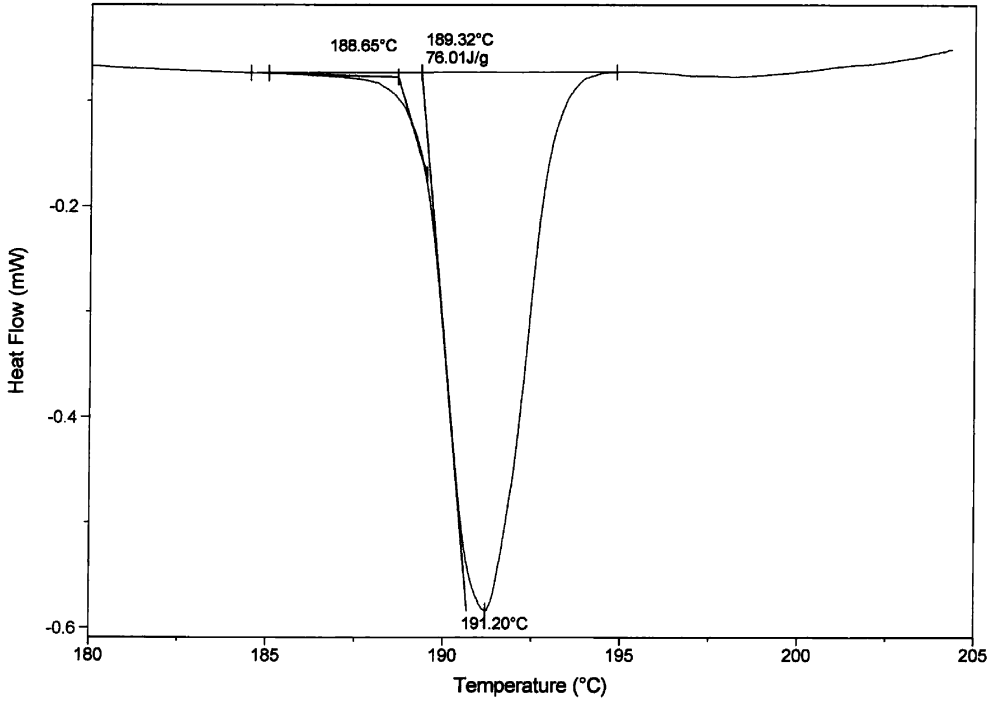

Figure 7. DSC thermogram associated with eutectic melting of a δ-HMX/S-RDX mixture.

eutectic melting event. None of the thin film photomicrographs obtained during these HSM operations are presented due to their poor quality.

Discussion

Two polymorph modications of the military grade HMX were observed during this investigation: β and δ with the transition from one polymorph to the other (β to δ) occurring in the 195–199°C temperature range at a DSC heating rate of 5°C/min and at 189.8°C at 1°C/min. This transition temperature showed some variation at the 5°C/min heating rate, for instance, the average peak temperature associated with sample weights of 0.2 and 7/9 mg was 198.4 ± 0.3°C, while that for sample weights of 0.9 and 1.6 mg was 195.4 ± 0.3°C. Also, the DSC thermogram associated with the sample weighing 0.9 mg exhibited a shoulder at 187.4°C. This variation in transition temperature and the observation of a shoulder with one sample may be the result of some RDX contamination that was introduced during production. It is pointed out, however, that all DSC samples of neat β-HMX used during these heating operations were obtained from the same sample container. The S-RDX exhibited a consistent, sharp melting temperature of 205.3°C.

This complex system is characterized by two binary eutectics, ideal behavior by the S-RDX component and thermal instability that is associated with liquid RDX and with excess solid δ-HMX in the presence of liquid RDX. The melting temperatures associated with the two eutectics are governed by HMX polymorphism with the one melting at the lower temperature (188.5°C) involving β-HMX and S-RDX and the one melting at the higher temperature (191.4°C) involving δ-HMX and S-RDX. This conclusion is supported by the single heating operation with δ-HMX and 57.1 mol% S-RDX that yielded a single eutectic melting event at an average temperature of 191.1°C followed by thermal decomposition at 196.4°C. These two eutectic compositions are hereinafter designated β-HMX{RDX}:RDX{β-HMX} and δ-HMX{RDX}:RDX{δ-HMX}, respectively. Brackets indicate solid solubility. The S-RDX component exhibits ideal behavior in that its melting characteristics are consistent with its calculated liquidus curve regardless of the number of remelting operations to a maximum temperature that is below that of S-RDX melting. This is supported by the data from the mixtures containing 92.3 and 96.8 mol% S-RDX that were subjected to three

melting operations to maximum temperatures of 195 and 190.5°C, respectively, cooled to ambient temperature, then heated again to thermal decomposition. The initial eutectic melting event at 188.5°C for the 92.3 mol% S-RDX was completely shifted to 191.7°C by the third remelting operation with no effect on the S-RDX melting temperature, 199.2°C (199.5°C during a single (initial only) melting operation, 200.4°C calculated), that was observed during the third remelting operation. The sample with 96.8 mol% S-RDX yielded an S-RDX melting temperature of 202.9°C (202.9°C during a single (initial only) melting operation, 203.3°C calculated) during the third remelting operation.

The calculated S-RDX liquidus curve crosses the average temperatures associated with the β-HMX{RDX}:RDX{β-HMX} and δ-HMX{RDX}:RDX{δ-HMX} eutectics at S-RDX compositions of 75.5 and 79.3 mol%, respectively. The former is consistent with the DSC thermograms associated with initial melting operations in that the endothermic events observed for the mixtures with 71.3 and 80.1 mol% S-RDX exhibit a slight tail, suggesting the presence of excess β-HMX in the case of the former composition and excess S-RDX in the case of the latter. The endothermic event observed for the mixture with 74.9 mol% S-RDX was symmetrical and was followed by an exothermic event at approximately 195°C. This same composition (74.9 mol% S-RDX), the composition presumed to be at or near the eutectic, was completely melted by 190°C when subjected to an HSM heating operation.

The thermal stability observed with mixtures rich in S-RDX ($>$ 79.5 mol%) is attributed to the lack of excess δ-HMX in the solid state after the δ-HMX{RDX}:RDX{δ-HMX} eutectic melts. It is believed that during the cooling/remelting operations the liquid HMX from the initial β-HMX{RDX}:RDX{β-HMX} eutectic melt recrystallizes completely to δ-HMX by the second or third remelting operation. As the β-HMX transitions to the δ-polymorph, the δ-HMX{RDX}:RDX{δ-HMX} eutectic forms preferentially over the β-HMX{RDX}:RDX{β-HMX} eutectic in the subsequent melting operations. At S-RDX concentrations greater than 79.5 mol% there will be no excess solid δ-HMX after the transition from one eutectic composition to the other, hence, the system is thermally stable until the excess solid S-RDX melts along its liquidus curve. At concentrations of S-RDX less than 79.5 mol% there will be an increasing concentration of solid δ-HMX that reaches a maximum at 75.5 mol% S-RDX and then decreases as the concentration of S-RDX decreases, as depicted in Figure 8. In fact, at

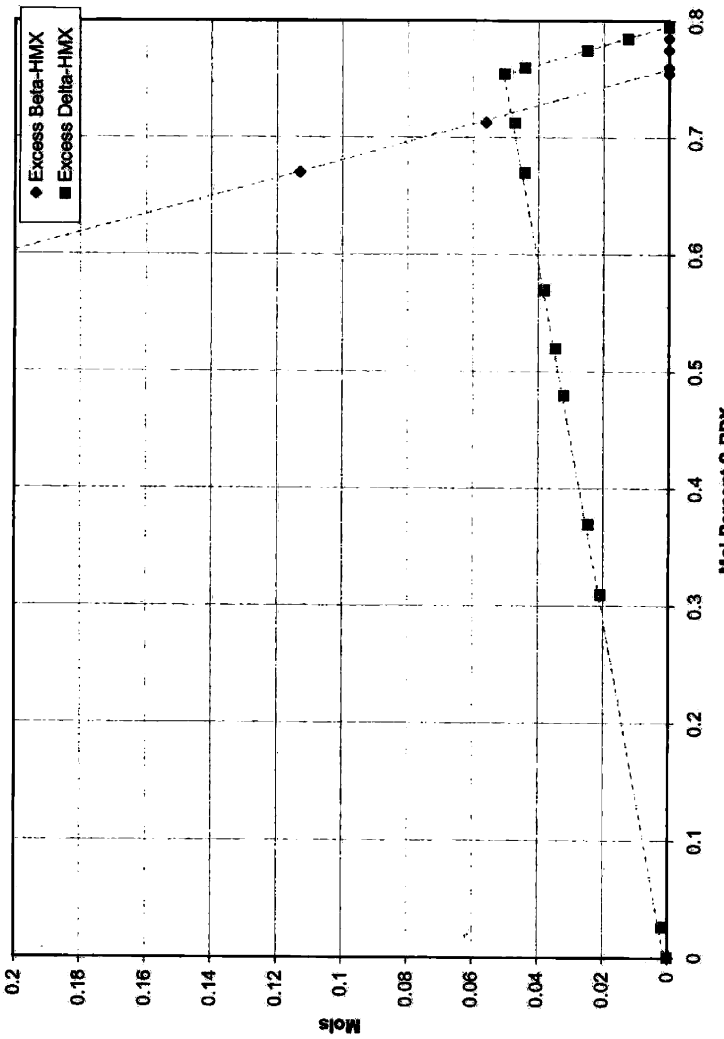

Figure 8. β- and δ-HMX depletion/formation diagram.

concentrations of S-RDX less than 75.5 mol% only a constant 79.5% of the maximum δ-HMX that can be formed is consumed in the δ-HMX:S-RDX eutectic composition. It is believed it is the presence of this excess solid δ-HMX that destabilizes the mixtures after successive melting operations. The end product of this destabilization is exothermic decomposition that initiates in the 195–196°C temperature range. During initial melting operations, destabilization of mixtures with S-RDX concentrations less than 75.5 mol% does not occur until the excess solid β-HMX transitions to the δ-polymorph at approximately 12–15°C after the β-HMX{RDX}:RDX{β-HMX} eutectic melts. The abrupt increase in this transition temperature from 198.6°C for neat β-HMX to the temperature range 201.5–203.2°C between 0 and 2.66 mol% S-RDX is attributed to the solid solubility of RDX in β-HMX. The tie line depicting this solid-state transition from β-HMX{RDX} to δ-HMX{RDX}, shown in Figure 4, is believed to extend to approximately 50 mol% S-RDX where it defines the intersection of the notional β-HMX and δ-HMX liquidus lines. Also shown in Figure 4 are the notional solidus lines depicting the transition from pure β- to δ-HMX. The data points at 2.66, 52.3, and 57.1 mol% S-RDX are tentatively labeled β-HMX{RDX} to δ-HMX{RDX} transition temperatures for lack of more definitive data. Endothermic processes that may have occurred between β-HMX{RDX}:RDX{β-HMX} eutectic melting and the initiation of thermal decomposition for mixtures with 66.8 and 71.3 mol% S-RDX were not sufficiently strong to be distinguished from the baseline.

The placement of the δ-HMX liquidus curve calculated by using the literature heat of fusion, while not consistent with the experimental data, suggested the existence of an δ-HMX:RDX eutectic at 92.3 mol% S-RDX and 200.4°C. This is consistent with thermal data acquired from neat HMX in that δ-HMX does not exist until the β to δ solid-state transition at 198°C. This β to δ transition, however, is postulated to occur at a lower temperature in the presence of RDX, that is, during the recrystallization of the β-HMX:S-RDX eutectic melt.

The formation of the β-HMX{RDX}:RDX{β-HMX} eutectic during initial melting operations explains the broad, usually twin-peaked endothermic event associated with HRDX immediately preceding thermal decomposition. The HRDX contains β-HMX, which will form the β-HMX{RDX}:RDX{β-HMX} eutectic that will melt in the 188–190°C temperature range followed by RDX melting at a temperature consistent with the HMX content.

Conclusions

Temperature/composition diagrams for the β-HMX/S-RDX and δ-HMX/S-RDX binary systems have been determined by using differential scanning calorimetry supported by limited hot stage microscopy. Both temperature/composition diagrams are signicantly affected by thermal decomposition primarily associated with the δ-HMX component and by solid solubility of RDX in both β- and δ-HMX. The S-RDX experimental liquidus temperatures and its computationally predicted liquidus curve were in close agreement. Two polymorphic modications associated with the neat HMX component, β and δ, were observed experimentally and conrmed by powder X-ray diffraction analysis. The intersection of the calculated RDX and δ-HMX liquidus curves, the latter calculated by using literature data for pure HMX, predicted a eutectic composition/melt-melting temperature that was not consistent with experimental eutectic data. Experimentally, two eutectic systems were observed, β-HMX{RDX}:RDX{β-HMX} and δ-HMX{RDX}:RDX{δ-HMX}, with average melting temperatures of 188.5 ± 0.3 and 191.4 ± 0.4°C, respectively, and with compositions in the ranges 74.9–75.5 and 79.0–79.3 mol% S-RDX, respectively. A heat of fusion that allowed the calculation of a δ-HMX liquidus curve that t the experimental data was calculated by using the melting temperature and composition associated with the δ-HMX/S-RDX eutectic system and the literature δ-HMX melting temperature. Unfortunately, no experimental δ-HMX melting temperatures were acquired to support the position of this liquidus curve due to the thermal instability of the excess solid δ-HMX that was formed upon recrystallization of the previously melted β-HMX{RDX}:RDX{β-HMX} eutectic.

Acknowledgments

We thank Dr. Ronald Armstrong of this laboratory for his comments and suggestions regarding this work, Wayne Richards for carrying out the XRD experiments, and Russ Huffman for carrying out all DSC experiments.

References

[1] Cady, H. H., and Smith, L. C. 3, May 1962. LAMS-2652. Los Alamos Scientific Laboratory, Los Alamos, NM.
[2] Brill, T. B., and Karpowicz, R. J. 1982 *J. Phys. Chem.* 86:4260.

[3] Landers, A. G., and Brill, T. B. 1980. *J. Phys. Chem.* 84:3573.
[4] Goetz, F., and Brill, T. B. 1979. *J. Phys. Chem.* 83(3):340.
[5] Krawietz, T. R., McKenney, R. L., Jr., and Ortiz, R. J. In press. Characterization of the unconfined slow cook-off response of nitramines and nitramine composites with TNT. *12th Int. Detonation Symp. Proc.,* San Diego, CA, 11–16 August 2000.
[6] McKenney, R. L., Jr., and Krawietz, T. R. July 1999. One-liter Test: A mid-scale safety characterization test for melt-castable explosives. AFRL-MN-EG-TR-1999–7049. Air Force Research Laboratory. Munitions Directorate. Distribution Unlimited. Eglin AFB, FL.
[7] Ciller, J. A., and Quintana, J. R. 1990. Influence of RDX on the thermal behavior of HMX. *21st International Annual Conference of ICT*, 55–1. Karlsruhe, Germany, July 3–6.
[8] Gibbs, T. R., and Popolato, A. (eds). 1980. *LASL Explosives Properties Data.* Berkeley: University of California Press.
[9] Batty, W. E., and Gilbert, B. October, 1959. The chemistry of RDX and HMX. ERDE 7/R/59.
[10] Chute, W. J., Downing, D. C., McDay, A. F., Myers, G. S., and Wright, G. F. 1949. *Can. J. Res.* 27B:218.
[11] Johnson, J. R. July 15, 1942. Crystallographic studies of RDX, HMX and related compounds. OSRD-6994.
[12] NIST. July 2001 Release. Standard Reference Database. No. 69.
[13] Meyer, R., 1977. *Explosives.* New York: Verlag Chemie.
[14] Herrmann, M., Engel, W., and Eisenreich, N. 1992. *Propellants, Explosives, Pyrotechnics* 17:190–195.
[15] JCPDS–ICDD Database, 2002 Release. PDF–2.